

## Article

# Composition and Textural Characteristics of Char Powders Produced by Thermomechanical Processing of Sunflower Seed Husks

Sergey M. Frolov <sup>1,\*</sup>, Anton S. Silantiev <sup>1</sup>, Ilias A. Sadykov <sup>1</sup>, Viktor A. Smetanyuk <sup>1</sup>, Fedor S. Frolov <sup>1</sup>, Yaroslav K. Hasiak <sup>1</sup>, Tatiana V. Dudareva <sup>1</sup>, Valentin G. Bekeshev <sup>1</sup>, Maksim V. Grishin <sup>1</sup>, Evgeniy K. Golubev <sup>1,2</sup>, Dinara Baimukhambetova <sup>1</sup>, Vera Ya. Popkova <sup>1</sup>, Alexander I. Vezentsev <sup>3</sup>, Alexander E. Razdobarin <sup>3</sup>, Maxim N. Yaprntsev <sup>3</sup> and Pavel V. Sokolovskiy <sup>2,4</sup>

- <sup>1</sup> Federal Research Center for Chemical Physics of the Russian Academy of Sciences (FRC), 119991 Moscow, Russia; silantevu@mail.ru (A.S.S.); ilsadykov@mail.ru (I.A.S.); smetanuk@mail.ru (V.A.S.); yanadva@mail.ru (T.V.D.); bekeshv@chph.ras.ru (V.G.B.); grishin@chph.ras.ru (M.V.G.); jeckagolubev@gmail.com (E.K.G.); vera.popkova@chph.ras.ru (V.Y.P.)
- <sup>2</sup> Enikolopov Institute of Synthetic Polymeric Materials, Russian Academy of Sciences, 117393 Moscow, Russia; levap90@list.ru
- <sup>3</sup> Department of General Chemistry, National Research University "Belgorod State University" (BSU), 308015 Belgorod, Russia; vesentsev@bsu.edu.ru (A.I.V.); 1046335@bsu.edu.ru (A.E.R.); yaprintsev@bsu.edu.ru (M.N.Y.)
- <sup>4</sup> N. D. Zelinsky Institute of Organic Chemistry, Russian Academy of Sciences, 119991 Moscow, Russia
- \* Correspondence: smfrol@chph.ras.ru



**Citation:** Frolov, S.M.; Silantiev, A.S.; Sadykov, I.A.; Smetanyuk, V.A.; Frolov, F.S.; Hasiak, Y.K.; Dudareva, T.V.; Bekeshev, V.G.; Grishin, M.V.; Golubev, E.K.; et al. Composition and Textural Characteristics of Char Powders Produced by Thermomechanical Processing of Sunflower Seed Husks. *Powders* **2023**, *2*, 624–638. <https://doi.org/10.3390/powders2030039>

Academic Editor: Paul Luckham

Received: 17 March 2023

Revised: 10 August 2023

Accepted: 6 September 2023

Published: 12 September 2023



**Copyright:** © 2023 by the authors. Licensee MDPI, Basel, Switzerland. This article is an open access article distributed under the terms and conditions of the Creative Commons Attribution (CC BY) license (<https://creativecommons.org/licenses/by/4.0/>).

**Abstract:** The paper presents the results of experimental studies on the production of fine char powder from sunflower seed husks by a novel method of thermomechanical treatment with pulsed shock waves and supersonic jets of the mixture of ultra-superheated (above 2000 °C) steam and carbon dioxide, as well as the results of examination of the produced char powder in terms of its chemical, phase, and granulometric composition and structural, morphological, and texture characteristics. The objective of the research is to explore the possibility of using the resulting char powder as a sorption-active material for organic substances. It is shown that the obtained char particles and their agglomerates have an average size of 20–30 nm and 12–24 μm, respectively, have the shape of disks and ellipsoids, consist mainly of amorphous carbon (up to 56 wt%) and oxygen (up to 42 wt%), and have a specific surface area of 1.1–1.7 m<sup>2</sup>/g. It is concluded that such a char powder can be used as an absorbent for organic substances when dried and deagglomerated.

**Keywords:** pulsed detonation gun; ultra-superheated steam and carbon dioxide; agricultural waste; waste recycling; sunflower seed husk; char powder; material composition; adsorbent

## 1. Introduction

Waste disposal is a complex scientific, technical, and socio-economic problem on a global scale [1–3]. Emissions from industrial enterprises and landfills pollute the atmospheric air, soil, and water bodies. Despite the great recent progress in waste management, the problems of reducing the negative impact of waste on the environment still require both scientific and practical solution. One of the existing problems is the utilization of sunflower seed husks, a waste product of the oil and fat food industry. On the territory of Russia there are more than 400 oil-producing enterprises with a capacity of 50 to 3000 ton per day; the daily volume of supplied oilseeds is 1000–1500 ton and enterprises separate 100–120 ton of sunflower seed husks per day [4] together with other byproducts [5,6]. Thus, a search for the optimal method of the utilization of sunflower seed husks that would meet economic and environmental requirements is undoubtedly an important scientific and practical problem.

The most promising solution to the problem is the thermal treatment of waste, accompanied by the partial recovery of energy and material resources. The environmental impact of the thermal treatment technologies is relatively small and is caused by gas and flying ash emissions as well as the generation of liquid tar and solid residues. The available thermal treatment technologies include direct combustion, pyrolysis, gasification, and their combinations [7–11]. The solid residues (ash powders) generated during combustion, pyrolysis, and gasification processes of sunflower seed husks are used as adsorbents for remediation of water or industrial liquid effluents [12,13] in the ceramic industry [14], in the iron ore sintering process [15], and as a filler for epoxy-based composites [16]. The smallest impact on the environment is produced by high-temperature gasification technologies based on the use of superheated water or superheated steam [17–19] and/or CO<sub>2</sub> [20], especially when the heat required for processing is obtained using environmentally friendly sources [21–23] other than the direct combustion of feedstock. The use of H<sub>2</sub>O or CO<sub>2</sub> as gasifying agents has a number of advantages [24,25]. Steam and carbon dioxide consist only of H and O atoms and C and O atoms, respectively, therefore, the syngas (a mixture of H<sub>2</sub> and CO) obtained during the gasification of organic waste is not diluted with other gases. Waste gasification with H<sub>2</sub>O and/or CO<sub>2</sub> requires less gasifying agent due to their high enthalpy. The use of a combined H<sub>2</sub>O/CO<sub>2</sub> gasifying agent makes it possible to control the composition of the syngas. The use of H<sub>2</sub>O as a gasifying agent increases the economic efficiency. Finally, syngas obtained by gasification in the absence of free oxygen does not contain such toxic compounds as dioxins and furans. The amount of H<sub>2</sub> obtained during the steam-assisted gasification of biomass is about three times greater than during its air-assisted gasification. Carbon dioxide, for the gasification of organic waste, can be taken from the flue gases of power plants, which will reduce greenhouse gas emissions and reduce the carbon footprint. Particularly attractive is the high-temperature steam gasification of organic waste which is carried out at temperatures above 1200 °C. In this case, the gasification products are the high-quality syngas and slag and the syngas consists mainly of H<sub>2</sub> and CO. The content of hydrocarbons above C<sub>1</sub>–C<sub>2</sub> is negligible and compounds containing alkali metals, chlorine, and sulfur take on the simplest chemical structures.

In [26–28], a novel technology for the utilization of organic wastes by the high-temperature gasification was proposed and implemented on the laboratory scale. It consists in the conversion of a condensed organic matter into a gaseous state by applying the gasifying agent represented by the mixture of ultra-superheated steam and carbon dioxide generated by pulsed detonations of a fuel–oxygen mixture. This technology is referred to as the pulsed detonation gun (PDG) technology. Using the PDG technology, it is possible to produce not only high-quality syngas [29–31] but also other target products like ultrafine char powders by controlling the flow rate and temperature of the gasifying agent.

There are two objectives of this work. The first objective is to explore the possibility of obtaining a fine char powder from sunflower seed husks by the novel technology of thermomechanical treatment with pulsed shock waves and jets of the mixture of ultra-superheated (above 2000 °C) steam and carbon dioxide. This powder is intended as a sorption-active material for organic substances. The second objective is to characterize the produced char powder in terms of its composition as well as its structural, morphological, and textural properties for assessing the possibility of its use as an adsorbent for organic substances. To achieve this latter objective, the various analytical methods were used in the work: energy dispersive analysis [32], scanning electron microscopy [33], X-ray diffractometry [34], wet laser diffraction [35], sorption analysis [36], and scanning probe microscopy (SPM) [37].

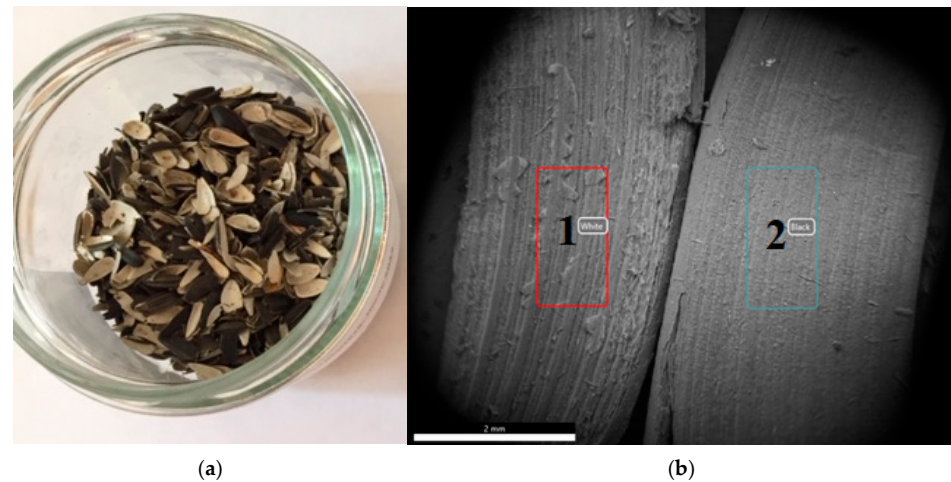
## 2. Materials and Methods

### 2.1. Feedstock

The sunflower seed husks correspond to the sunflower variety Belgorodsky 94 and consist of approximately 48.4% cellulose, 34.6% hemicellulose, and 17% lignin [38]. The moisture of the sunflower seed husks was 9.95–10.00 wt%. To determine the chemical

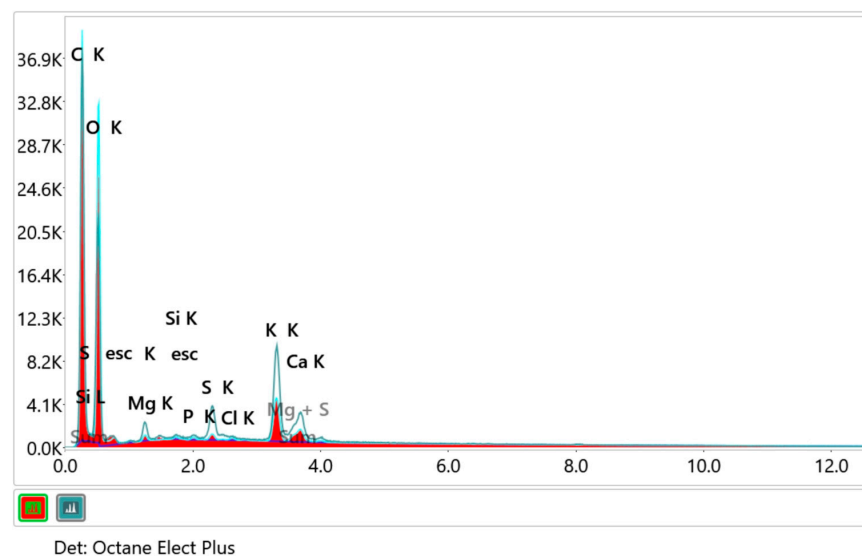
composition of the husks, scanning electron microscopy was carried out in conjunction with the energy dispersive analysis in the same zones of a sample.

Figure 1 shows the photograph of the feedstock (Figure 1a), the microphotographs of the fibrous structure, and the relief of the original feedstock material in two chosen zones 1 and 2 (Figure 1b).



**Figure 1.** Sunflower seed husks: (a) original feedstock and (b) material fibrous structure and relief. Zones 1 and 2 are the locations where the chemical composition of the feedstock was determined.

Figure 2 shows the energy-dispersive spectrum of the feedstock. High responses of oxygen and carbon are recorded with smaller responses of potassium and calcium. Table 1 shows the chemical composition of sunflower seed husks. In addition to oxygen (48–54 wt%), carbon (45–47 wt%), potassium (1.0–2.4 wt%), and calcium (0.3–0.9 wt%), there is some magnesium (0.2–0.7 wt%), sulfur (0.1–0.7 wt%), phosphorus (0.05–0.07 wt%), silicon (0.04wt%), and chlorine (0.04–0.05 wt%). Table 2 shows the compositions of natural gas used as a fuel in the PDG. The purity of technical oxygen used as an oxidizer in the PDG was 99.7%. The composition of the natural gas–oxygen mixture used in the PDG was close to stoichiometric (fuel-to-oxygen equivalence ratio 1.1): it was chosen to avoid the presence of free oxygen in the detonation products. Table 3 shows the composition of the gasifying agent—the mixture of ultra-superheated steam and carbon dioxide—measured in the experiments without a feedstock supply.



**Figure 2.** Energy-dispersive spectrum of sunflower seed husks.

**Table 1.** Chemical composition of sunflower seed husks.

Point 1 in Figure 1b		Point 2 in Figure 1b	
Element	wt%	Element	wt%
O	53.50	O	48.18
C	44.75	C	46.93
K	0.99	K	2.43
Ca	0.31	Ca	0.86
Mg	0.21	Mg	0.73
S	0.11	S	0.69
P	0.05	P	0.07
Si	0.04	Si	0.04
Cl	0.04	Cl	0.05

**Table 2.** Compositions of natural gas.

Species	vol%
CH <sub>4</sub>	96.1
C <sub>2</sub> H <sub>6</sub>	2.1
C <sub>3</sub> H <sub>8</sub>	0.6
C <sub>4</sub> H <sub>10</sub>	0.2
N <sub>2</sub>	1.0

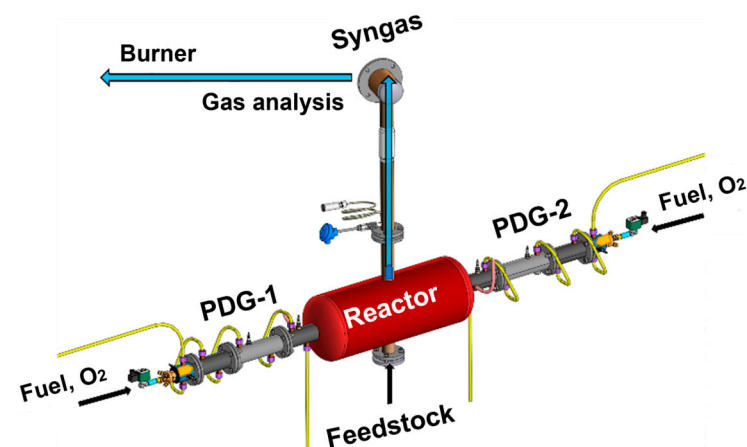
**Table 3.** Composition of the gasifying agent.

Species	vol%
H <sub>2</sub> O	65
CO <sub>2</sub>	32
CO	2
H <sub>2</sub>	1

Remark: measured by flow gas analyzer MRU VARIO SYNGAS PLUS (Germany), the measurement error of volume fractions is estimated at 5%.

## 2.2. Feedstock Gasifier

Figure 3 shows a schematic of a feedstock gasifier (FG). The FG consists of two coaxial identical PDGs (PDG-1 and PDG-2) attached from opposite sides to the flow reactor. Solid feedstock is loaded into the reactor in batches or fed continuously with a screw feeder through an opening in the bottom of the reactor. The description of the design and operation principle of the PDG, flow reactor, and FG, as a whole, is given below.

**Figure 3.** Feedstock gasifier.

The PDG is a water-cooled tube with a diameter of 50 mm and a length of 0.63 m with one open and the other closed end. The open end of the tube communicates with

the flow reactor. The closed end of the tube is equipped with a spark plug and ports for supplying fuel (natural gas) and oxygen from manifolds with control valves. After the mixture is ignited by a spark plug, the flame is accelerated until the deflagration-to-detonation transition occurs and the resulting detonation wave propagates through the mixture at a speed above  $\sim 2000$  m/s. The detonation wave converts the initial mixture into the detonation products, consisting mainly of  $H_2O$  and  $CO_2$  (see Table 3) with very high values of temperature (above  $3400$  °C) and pressure (above 20 bar). After the generated shock wave enters the flow reactor, the detonation products expand into the flow reactor in the form of a high-speed (above 1000 m/s, on average) jet. When the pressure in the PDG drops to the atmospheric pressure, a new portion of fuel and oxygen is fed to the PDG through the ports at the closed end. After the PDG is filled with the mixture, the spark plug ignites the mixture and the next operation cycle begins, i.e., the PDG operates in a pulsed mode with a pulse frequency mainly determined by the tube fill time.

The flow reactor with a volume of  $40\text{ dm}^3$  has a compact geometric shape to avoid the formation of long-lived gas-dynamic stagnation zones leading to feedstock accumulation and slagging. Two PDGs are connected to the flow reactor coaxially opposite to each other to create strong colliding incident shock waves and powerful vortex structures increasing the residence time of feedstock particles inside the flow reactor. Pulsed shock waves emanating from the PDGs possess a tremendous destructive power. On the one hand, they effectively crush the feedstock. On the other hand, they prevent the agglomeration of feedstock particles and their adhesion to the walls of the flow reactor during FG operation. It is worth noting that feedstock particles can be subjected to multiple acts of fragmentation by successive incident and reflected shock waves and can be repeatedly involved in the powerful vortex structures of the high-temperature gasifying agent far from relatively cold walls during their stay in the flow reactor. The flow reactor is also equipped with outlet ports for the continuous outflow of syngas and the continuous or periodic removal of solid residue. The average operation pressure in the flow reactor is slightly higher than the atmospheric pressure in order to avoid the suction of atmospheric air.

The operation principle of the FG includes two transient stages before reaching the nominal operation mode. After the first transient stage, the FG reaches a stationary operation mode with a steady thermal state of all its elements and cooling water. At this stage, the feedstock is not fed into the flow reactor. Thereafter, the second transient stage begins with feeding the feedstock into the flow reactor. After some time, the nominal operation mode of the FG is established with a new steady thermal state of all its elements and cooling water, as well as with the steady composition of the produced syngas. The parameters of the gasifying agent entering the flow reactor and the quality of the produced syngas are controlled by the PDG fill and operation frequency as well as by the mass flow rate of feedstock. The maximum operation frequency achieved with the full fill of the PDGs was 3 Hz. Under such conditions, complete gasification of sunflower seed husks was achieved without the formation of tar and char. With decreasing the PDG fill and the operation frequency, the average temperature of the gasifying agent in the flow reactor was decreasing and the efficiency of the gasification process was worsening. The efficiency worsening means a decrease in the yields of  $H_2$  and  $CO$  and an increase in the yields of  $CH_4$ , higher hydrocarbons, and  $CO_2$  in the produced syngas as well as the detection of solid residue (fine char). The latter is the subject of interest in this work. It is worth noting that the gasification of feedstock in the FG proceeds at a local instantaneous temperature in the flow reactor (which exceeds  $2000$  °C) rather than at the average temperature. Nevertheless, the measured level of the average temperature in the flow reactor reflects the characteristic time of the impact of the high-temperature gasifying agent on the feedstock: the lower the average temperature, the shorter the characteristic time of gasification. It is also worth noting that the char powder thus obtained can be subject to wetting and agglomeration after the termination of thermomechanical treatment in the FG due to steam condensation. The latter implies the possible need for additional drying and fragmentation operations for the char powder.

### 2.3. Energy Dispersive Analysis and Scanning Electron Spectroscopy

The elemental composition of the studied samples of char powder is determined by the method of energy dispersive analysis, which is carried out in conjunction with scanning electron microscopy. For this purpose, the Nova NanoSEM analytical system is combined with a high-resolution scanning electron microscope Quanta FEG. The device is equipped with an EDAX analytical energy-dispersive spectrometer, which is capable of determining the elemental composition of substances in different areas of the sample and revealing graphic dependences and maps of the distribution of elements over the surface in the sample under study when placed in the magnetic field of an objective lens, which makes it possible to reduce aberration and achieve sub nanometer resolution. This mode is suitable for studying nonmagnetic samples. It is also worth noting that the Nova NanoSEM analytical system is equipped with an intralens secondary electron detector that provides high detail of the near-surface region of a sample. No special preparation of a sample before analysis is required. The measurements were carried out in the Center for collective use “Technologies and Materials of the National Research University” BSU.

### 2.4. X-ray Diffractometry

Chemical analysis helps to reveal the phase composition of the sample under study. The phase composition of char powder obtained from sunflower seed husks is determined using a SmartLab X-ray diffractometer (Rigaku, Tokyo, Japan). The diffractometer is equipped with a high-speed D/tex Ultra Hi Pix detector. In this analysis, the pseudo-parallel beam is focused following the Bragg-Brentano procedure. The interpretation of X-ray powder diffraction patterns allows the identification of the phase composition of the analyzed material.

### 2.5. Particle Size Distribution

The particle size distribution in char powder is studied by a laser diffraction wet dispersion method on an Analysette 22 device (Fritch, Idar-Oberstein, Germany) in the presence of surfactants during ultrasonic treatment (50 W) and particle analysis using a scanning probe microscopy (SPM). For the laser diffraction wet dispersion method, specimens are prepared by rubbing with a spatula in a bottle with the addition of a surfactant. The operation of an atomic force microscope is based on the force interaction between the probe and the surface of the sample, which leads to a registered deformation of the probe-cantilever. The possibilities of AFM allow investigating the structure of almost any solid surface in vacuum, in a liquid, and “in air conditions” [39–44]. A review of modern achievements in the field of AFM can be found, e.g., in [45]. The use of SPM is explained by the unique resolution of this method, which makes it possible to conduct research at the atomic level. Unlike other types of electron microscopes, SPM does not require a high vacuum to operate. It can work in air and liquid media. The use of SPM makes it possible to reveal the features of the crystal structure of the surface and its roughness, to observe the patterns of nucleation during film growth, and to study viruses, DNA molecules, etc.

### 2.6. Specific Surface Area

The specific surface area of char powder was determined by the method of low-temperature nitrogen sorption at 77 K. The measurements were carried out on a NOVA 1200e gas sorption analyzer (Quantachrome Instruments, Boynton Beach, FL, USA). Highly purified nitrogen gas was used as the adsorbate. Before measurements, the sample was degassed in a vacuum at 200 °C for 2 h.

## 3. Results and Discussion

Using the new PDG technology of thermomechanical treatment of organic feedstock with pulsed shock waves and jets of the mixture of ultra-superheated (above 2000 °C) H<sub>2</sub>O and CO<sub>2</sub>, three samples of char powder are obtained from sunflower seed husks in three

experiments under approximately the same experimental conditions (average temperature of the walls of the flow reactor of 400–450 °C; atmospheric pressure; a feedstock batch of 2 kg). These samples are taken from the flow reactor after the termination of FG operation and when it is cooling down and are further studied by the various analytical methods at the FRC and BSU. For the sake of brevity, we describe the results obtained for only one of the samples (Figure 4) below.



**Figure 4.** A sample of char powder produced by the PDG technology.

Figure 5 and Table 4 show the energy-dispersive spectrum and proximate analysis of char powder obtained by the thermomechanical treatment of sunflower seed husks.

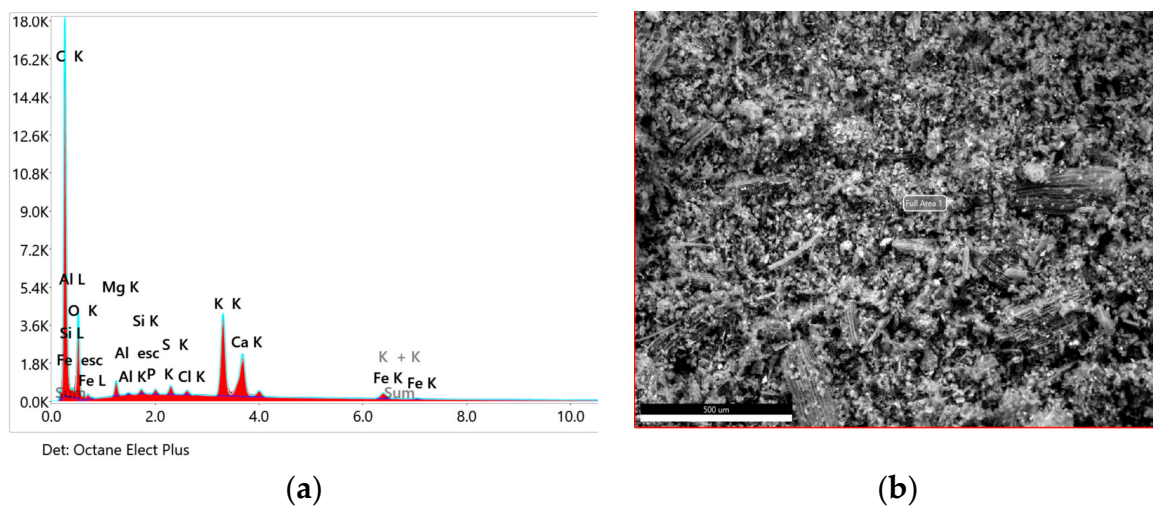


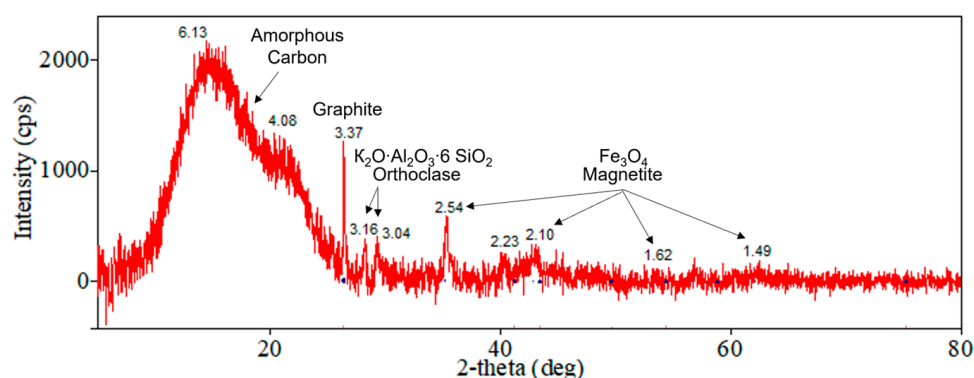
**Figure 5.** Energy-dispersive spectrum of char powder obtained by the thermomechanical treatment of sunflower seed husks: (a) energy dispersive spectrum and (b) electron microphotograph with a zone (“Full Area 1”) where the energy dispersive analysis was made.

**Table 4.** Proximate analysis of char powder.

Element	wt%
C	51.76
O	38.63
Mg	1.15
Al	0.10
Si	0.19
P	0.22
S	0.35
Cl	0.20
K	4.18
Ca	2.58
Fe	0.65

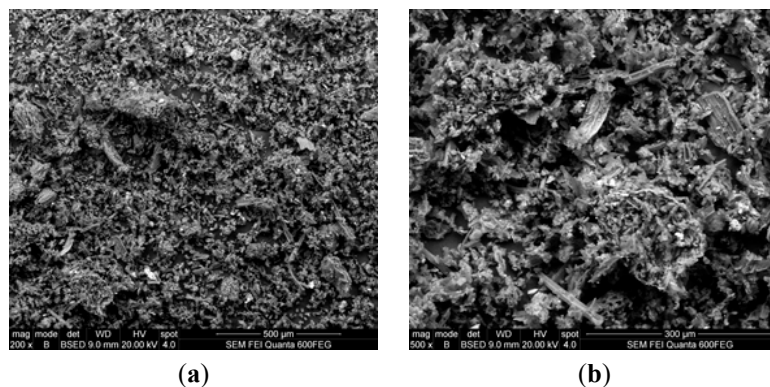
As seen from Table 4, the content of carbon increased from 45–47 wt% in the original feedstock to about 52 wt% in the char, whereas the content of bound oxygen decreased from 48–54 wt% in the original feedstock to about 39 wt% in the char. As compared to the original feedstock, the content of potassium, calcium and magnesium increased considerably and attained 4.2, 2.6, and 1.2 wt%, respectively. The presence of iron in the char is most probably caused by the abrasive processes on the reactor walls during feedstock gasification.

Figure 6 shows the phase composition of char powder obtained by X-ray phase analysis indicating the presence an amorphous phase (soot), as well as graphite and magnetite. The amorphous phase is presumably composed of carbon. The appearance of the graphite phase is due to the harsh thermal conditions of the experiment. The magnetite phase could be formed during the oxidation of the material. The phases of orthoclase and microcline are also revealed. Their presence can be explained by the high content of potassium in the test sample, as shown by chemical analysis.



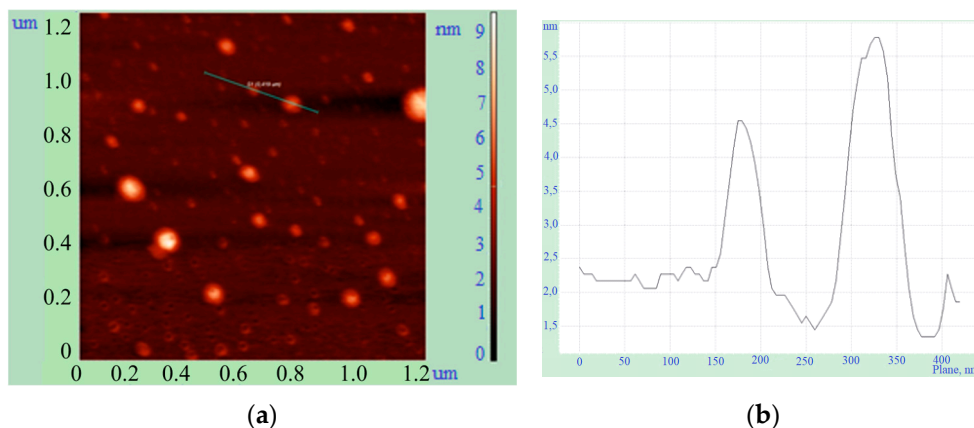
**Figure 6.** X-ray diffraction pattern of char powder obtained by the thermomechanical treatment of sunflower seed husks. Numerical values of interplanar distances are given in Å.

Figure 7 shows microphotographs of char powder obtained by the thermomechanical treatment of sunflower seed husks. Figure 7a shows white particles of various shapes and sizes ranging from 10 to 165  $\mu\text{m}$ . On large particles of 25 and 120  $\mu\text{m}$ , cellular pores 10  $\mu\text{m}$  in size were found. Figure 7b shows white particles ranging in size from 8 to 84  $\mu\text{m}$  and white tubular particles 170  $\mu\text{m}$  long and 25  $\mu\text{m}$  in diameter.



**Figure 7.** Electron microphotographs of char powder obtained by thermomechanical treatment of sunflower seed husks. Fragments (a,b) correspond to different parts of the sample.

Figures 8–10 show the results of char studies with the SPM. The char was deposited on the mica surface. Two groups of particles can be distinguished: “large” and “small”. The diameter of “large” particles was 100–150 nm at a thickness of 10–60 nm. Such particles can be either almost flat (“discs”) or have the shape of an ellipsoid. There are also “small” particles with a diameter of 20–50 nm and thickness of 1–4 nm. In their shape, particles of such sizes resemble pucks flattened to the edges. Particles of the average size range 20–30 nm make up the majority of the char particles in the sample.



**Figure 8.** “Large” and “small” particles. Results of examining a char sample with a scanning probe microscope: (a) image of the surface and (b) particle profile along the blue line.

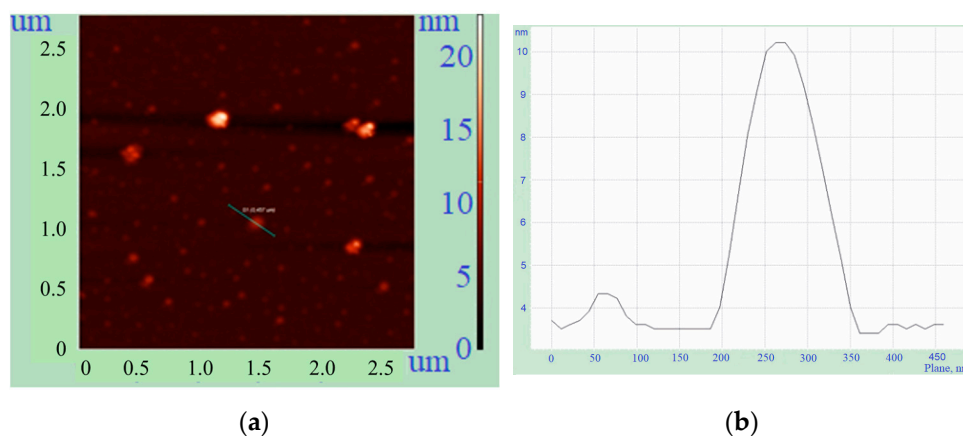


**Figure 9.** “Large” particles. Results of examining a char sample with a scanning probe microscope: (a) image of the surface and (b) particle profile along the blue line.

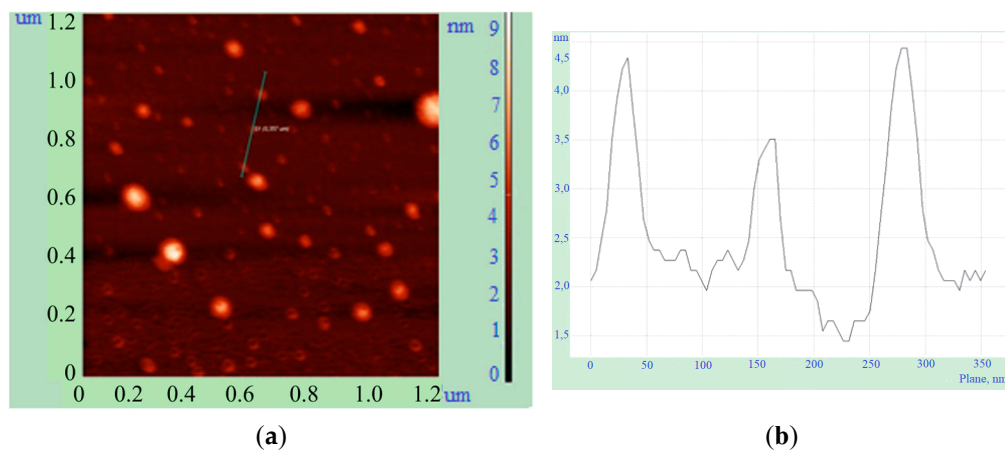


**Figure 10.** “Small” particles. Results of examining a char sample with a scanning probe microscope: (a) image of the surface and (b) particle profile along the blue line.

To obtain the particle size distribution of char particles by laser diffraction wet dispersion method, three specimens are taken from different places of the sample. The results are presented in Figure 11 and in Table 5 (average of three measurements for each specimen).

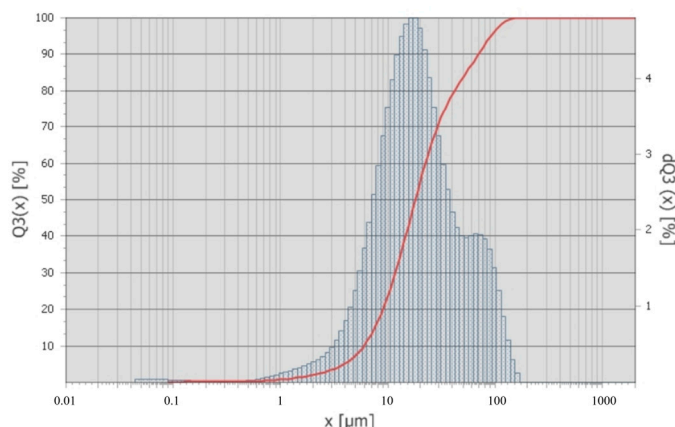


**Figure 11.** The example of the size distribution of char powder particles.

**Table 5.** Distribution of char particles by size (average of three measurements for each specimen).

Specimen	$D_{10}$ , $\mu\text{m}$	$D_{50}$ , $\mu\text{m}$	$D_{90}$ , $\mu\text{m}$
1	5.9	17.9	69.7
2	5.3	17.4	72.6
3	5.3	17.0	59.1

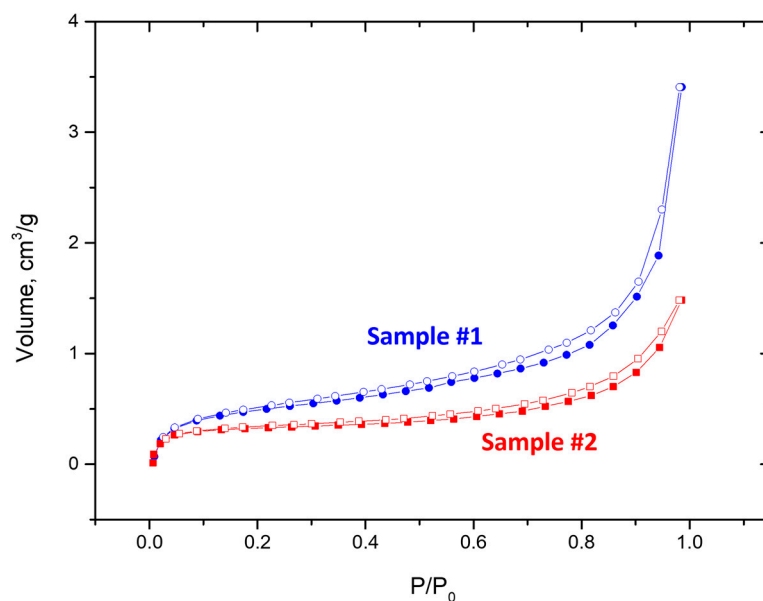
The study of particle size distribution allows the average particle size to be determined in each specimen: 19.35  $\mu\text{m}$  in specimen 1, 19.73  $\mu\text{m}$  in specimen 2, and 24.40  $\mu\text{m}$  in specimen 3. Thus, the char powder under study is composed of both single particles with sizes ranging from tens to hundreds of nanometers and their agglomerates with sizes ranging from tens to hundreds of micrometers.

Table 6 summarizes the data for particle size distribution for three samples of char powder obtained by thermomechanical treatment of sunflower seed husks (average values for each sample). The particle size distributions in the three samples are seen to differ essentially. Since these differences can be caused by the differences in the experimental conditions in terms of the reactor wall temperature (400–450 K), we do not provide the average values over the samples here.

**Table 6.** Particle size distributions for three samples of char powder obtained by the thermomechanical treatment of sunflower seed husks.

Sample	$D_{10}$ , $\mu\text{m}$	$D_{50}$ , $\mu\text{m}$	$D_{90}$ , $\mu\text{m}$
1	6.9	23.1	63.0
2	5.5	17.4	67.1
3	4.7	14.6	113.4

For determining the specific surface area of the three samples under study, the method of low-temperature sorption of gaseous nitrogen  $\text{N}_2$  at 77 K is used [46]. To exclude the release of toxic and contaminating substances during degassing, the samples are preliminarily dried in an oven for 2 h at a temperature of 150 °C. Then, the samples are degassed in a vacuum at a temperature of 200 °C for 2 h. Next, the specific surface area is measured. Figure 12 shows  $\text{N}_2$  adsorption and desorption isotherms at 77 K for Samples #1 and #2. The isotherms can be classified as type II according to the IUPAC classification [47,48], which is characteristic of nonporous or macroporous samples. The adsorption isotherm of Sample #1 shows a sharper increase in the region of high  $P/P_0$  values compared to the adsorption isotherm of Sample #2. This is due to the filling of macropores formed by large particles in Sample #1. Indeed, the microphotographs of Samples #1 and #2 show a more uniform pattern of smaller particles in Sample #2 than in Sample #1. This is also confirmed by the SPM data, which shows the presence of a greater number of “large” particles in Sample #1.

**Figure 12.** Isotherms of adsorption (filled symbols) and desorption (empty symbols) of nitrogen  $\text{N}_2$  at 77 K for samples #1 and #2 of char powder.

The specific surface area  $S_{BET}$  is determined by the Brunauer–Emmett–Teller (BET) method [49] in the relative pressure range  $P/P_0 = 0.05–0.30$  ( $P_0$  is the pressure of saturated vapors of the adsorbate at the experimental temperature). Unfortunately, we failed to obtain an adsorption isotherm suitable for processing for Sample #3. Apparently, this is due to the predominance of a large fraction of particles with an underdeveloped surface in Sample #3, which determines its low sorption capacity. Therefore, the specific surface area  $S_{BET}$  for Sample #3 is determined by the one-point method at  $P/P_0 = 0.30$ . The data obtained are presented in Table 7. As can be seen, the specific surface of the studied samples is different and low. The former can be caused by the differences in the experimental conditions in terms of the reactor wall temperature (400–450 K). Therefore, we do not provide the average values over the samples here. The latter indicates that the samples are dominated

by particles with an underdeveloped surface with no micro- and mesopores presumably due to both high process temperatures [50] and the presence of condensed moisture after the thermomechanical treatment. The SPM data and the data on particle size distribution imply that the samples are mainly composed of agglomerates of fine char particles that are 20–30 nm in average size. This means that further drying and fragmentation of the obtained char powder could significantly increase the specific surface, thus contributing to high sorption properties of the resultant char powder.

**Table 7.** Specific surface area of char powder particles of three samples obtained by the thermomechanical treatment of sunflower seed husks.

Sample	$S_{BET}$ , m <sup>2</sup> /g
1	1.7
2	1.1
3	1.4

Due to high process temperatures, the amorphous carbon (soot) obtained by the thermomechanical treatment of sunflower seed husks does not contain acidic oxygen-containing groups that could sorb metal ions by the ion exchange mechanism. Therefore, based on the results of this study, it can be concluded that the obtained char powder can be used (after drying and deagglomeration) as a sorption-active material primarily in relation to organic substances. It is also possible to improve the properties of the obtained sorbents: the number of pores can be increased, e.g., by chemical activation of the resulting sorbents.

#### 4. Conclusions

The paper describes the results of experimental studies on the production of fine char powder from sunflower seed husks by a novel method of thermomechanical treatment, namely, by pulsed shock waves and jets of the mixture of ultra-superheated (above 2000 °C) steam and carbon dioxide, as well as the results of studying char chemical, phase, and granulometric composition and its structural, morphological, and textural characteristics. The original feedstock exhibited a fibrous microstructure with uneven relief and contained mainly carbon (46 wt%) and oxygen (53 wt%) with minor concentrations of potassium, calcium, and magnesium. The gasifying agent was obtained by pulsed detonations (1 Hz) of near-stoichiometric natural gas–oxygen mixture and was composed of steam (62 vol%), carbon dioxide (35 vol%), and trace amounts of H<sub>2</sub> and CO.

Experiments showed that with a gradual decrease in the fill and operation frequency of a pulsed detonation gun, the average temperature in the gasifier with a loaded portion of sunflower seed husks gradually decreases leading to the appearance of a solid residue in the form of fine char particles in the gasification products. Three experiments were carried out on the gasification of sunflower seed husks with the production of char powder. The experiments slightly differed in the average gasification temperature (at the level of 400–450 K). Three samples of char powders were studied in terms of their material composition (chemical, phase, and granulometric) as well as structural, morphological, and textural characteristics. As compared to the original feedstock, the chars contained somewhat more carbon (51 to 56 wt%) and less oxygen (33 to 42 wt%) as well as increased concentrations of potassium (up to 5 wt%), calcium (up to 2.6 wt%), and magnesium (up to 1 wt%). The char powder contained both single particles and their agglomerates formed due to the agglomeration of particles in the course of steam condensation upon the completion of experiments. Single char particles had an average size of 20–30 nm, whereas their agglomerates had an average size of 12–24 μm. Due to the presence of particle agglomerates, the specific surface area of char powders was relatively low and equal to 1.1 to 1.7 m<sup>2</sup>/g. Nevertheless, when dried and deagglomerated, the obtained char powder can be used as a sorption-active material in relation to organic substances.

Thus, we have achieved the objective of the study and obtained a very fine char powder with particles of tens of nanometers in average size. Unfortunately, these particles

were agglomerated after the thermomechanical treatment due to the presence of condensed moisture. The future work will be aimed at fragmenting and drying the obtained char powder agglomerates by pulsed shock waves and jets of incondensable gas, e.g., nitrogen.

**Author Contributions:** Conceptualization, S.M.F. and A.I.V.; methodology, S.M.F., V.Y.P. and A.I.V.; investigation, A.S.S., I.A.S., V.A.S., F.S.F., Y.K.H., T.V.D., V.G.B., M.V.G., E.K.G., D.B., A.E.R., M.N.Y. and P.V.S.; resources, S.M.F., V.Y.P., and A.I.V.; writing—original draft preparation, S.M.F.; writing—review and editing, S.M.F.; supervision, S.M.F., V.Y.P. and A.I.V.; project administration, V.Y.P. All authors have read and agreed to the published version of the manuscript.

**Funding:** This work was partly supported by grant No. 4-19-01/160 for the provision of state support for the introduction of innovative technologies into production within the framework of a full-cycle technological project “Development of a technology for processing organic agricultural waste into adsorbents and backfill soils for landfills”.

**Institutional Review Board Statement:** Not applicable.

**Informed Consent Statement:** Not applicable.

**Data Availability Statement:** Data will be available on request.

**Conflicts of Interest:** The authors declare no conflict of interest.

## References

1. Rusakov, N.V.; Rakhmanin, Y.A. *Waste, Environment, Human; Medicine Publ.*: Moscow, Russia, 2004.
2. Giusti, L. A review of waste management practices and their impact on human health. *Waste Manag.* **2009**, *29*, 2227–2239. [[CrossRef](#)]
3. Goutam Mukherjee, A.; Ramesh Wanjari, U.; Chakraborty, R.; Renu, K.; Vellingiri, B.; George, A.; Valsala Gopalakrishnan, A. A review on modern and smart technologies for efficient waste disposal and management. *J. Environ. Manag.* **2021**, *297*, 113347. [[CrossRef](#)]
4. Smytchagin, E.O.; Mustafaev, S.K. Analysis of the composition of oil seed cleaning wastes and methods for their disposal and processing. *Sci. J. Kuban State Agric. Univ.* **2016**, *120*, 651–663.
5. Filho, J.G.; Egea, M.B. Sunflower seed byproduct and its fractions for food application: An attempt to improve the sustainability of the oil process. *J. Food Sci.* **2021**, *86*, 1497–1510. [[CrossRef](#)]
6. Fawzy, M.; Hassanien, R. (Eds.) *Bioactive Phytochemicals from Vegetable Oil and Oilseed Processing By-Products*; Springer: Cham, Switzerland, 2023. [[CrossRef](#)]
7. Higman, C.; Van der Burgt, M. *Gasification*, 1st ed.; Gulf Professional Publ.: Houston, TX, USA, 2005.
8. Rezaian, J.; Cheremisinoff, N. *Gasification Technologies. A Primer for Engineers and Scientists*, 1st ed.; CRC Press: Boca Raton, FL, USA, 2005.
9. Basu, P. *Biomass Gasification and Pyrolysis: Practical Design and Theory*; Academic Press: Burlington, MA, USA, 2010.
10. Turzynski, T.; Kluska, J.; Ochnio, M.; Kardaś, D. Comparative analysis of pelletized and unpelletized sunflower husks combustion process in a batch-type reactor. *Materials* **2021**, *14*, 2484. [[CrossRef](#)]
11. Spiewak, K.; Soprych, P.; Czernski, G. Influence of pressure and sunflower husks ash as catalyst on tire-char steam gasification. *Energy Rep.* **2023**, *9*, 1–15. [[CrossRef](#)]
12. Mohan, D.; Pittman, C., Jr. Activated carbons and low cost adsorbents for remediation of tri- and hexavalent chromium from water. *J. Hazard. Mater.* **2006**, *137*, 762–811. [[CrossRef](#)] [[PubMed](#)]
13. Nunes, A.; Franca, A.; Oliveira, L. Activated carbons from waste biomass: An alternative use for biodiesel production solid residues. *Bioresour. Technol.* **2009**, *100*, 1786–1792. [[CrossRef](#)]
14. Quaranta, N.; Unsen, M.; López, H.; Giansiracusa, C.; Roether, J.A.; Boccaccini, A.R. Ash from sunflower husk as raw material for ceramic products. *Ceram. Int.* **2011**, *37*, 377–385. [[CrossRef](#)]
15. Ooi, T.C.; Aries, E.; Ewan, B.C.R.; Thompson, D.; Anderson, D.R.; Fisher, R.; Fray, T.; Tognarelli, D. The study of sunflower seed husks as a fuel in the iron ore sintering process. *Miner. Eng.* **2008**, *21*, 167–177. [[CrossRef](#)]
16. Barczewski, M.; Sałasińska, K.; Szulc, J. Application of sunflower husk, hazelnut shell and walnut shell as waste agricultural fillers for epoxy-based composites: A study into mechanical behavior related to structural and rheological properties. *Polym. Test.* **2019**, *75*, 1–11. [[CrossRef](#)]
17. Zhan, L.; Jiang, L.; Zhang, Y.; Gao, B.; Xu, Z. Reduction, detoxification and recycling of solid waste by hydrothermal technology: A review. *Chem. Eng. J.* **2020**, *390*, 124651. [[CrossRef](#)]
18. Boukis, N.; Stoll, I.K. Gasification of biomass in supercritical water, challenges for the process design—Lessons learned from the operation experience of the first dedicated pilot plant. *Processes* **2021**, *9*, 455. [[CrossRef](#)]

19. DiCarlo, A.; Savuto, E.; Foscolo, P.U.; Papa, A.A.; Tacconi, A.; Del Zotto, L.; Aydin, B.; Bocci, E. Preliminary results of biomass gasification obtained at pilot scale with an innovative 100 kWth dual bubbling fluidized bed gasifier. *Energies* **2022**, *15*, 4369. [[CrossRef](#)]
20. Roncancio, R.; Gore, J.P. CO<sub>2</sub> char gasification: A systematic review from 2014 to 2020. *Energy Convers. Manag. X* **2021**, *10*, 100060. [[CrossRef](#)]
21. Oliveira, M.; Ramos, A.; Ismail, T.M.; Monteiro, E.; Rouboa, A. A review on plasma gasification of solid residues: Recent advances and developments. *Energies* **2022**, *15*, 1475. [[CrossRef](#)]
22. Chun, Y.N.; Song, H.G. Microwave-induced carbon–CO<sub>2</sub> gasification for energy conversion. *Energy* **2020**, *190*, 116386. [[CrossRef](#)]
23. Yi, F.; Manosh, C.P.; Sunita, V.; Xian, L.; Young-Kwon, P.; Siming, Y. Concentrated solar thermochemical gasification of biomass: Principles, applications, and development. *Renew. Sustain. Energy Rev.* **2021**, *150*, 11484. [[CrossRef](#)]
24. Frolov, S.M. Organic waste gasification: A selective review. *Fuels* **2021**, *2*, 556–651. [[CrossRef](#)]
25. Shahbeig, H.; Shafizadeh, A.; Rosen, M.A.; Sels, B.F. Exergy sustainability analysis of biomass gasification: A critical review. *Biofuel Res. J.* **2022**, *33*, 1592–1607. [[CrossRef](#)]
26. Frolov, S.M.; Smetanyuk, V.A.; Avdeev, K.A.; Nabatnikov, S.A. Method for Obtaining Highly Overheated Steam and Detonation Steam Generator Device (Options). Patent of Russian Federation No. 2686138, 24 April 2019. Priority dated 26 February 2018.
27. Frolov, S.M.; Smetanyuk, V.A.; Nabatnikov, S.A. Method of Gasification of Coal in a Highly Overheated Water Vapor and Device for Its Implementation. Patent of Russian Federation No. 2683751, 1 April 2019. Priority dated 24 May 2018.
28. Frolov, S.M.; Nabatnikov, S.A.; Diesperov, K.V.; Achildiev, E.R. Method for Decontamination of A Fly Ash Formed during Burning of Wastes and A Device for Its Implementation. Patent of Russian Federation No. 2739241, 22 December 2020. priority dated 11 June 2020.
29. Frolov, S.M. Organic waste gasification by ultra-superheated steam. *Energies* **2023**, *16*, 219. [[CrossRef](#)]
30. Frolov, S.M.; Smetanyuk, V.A.; Sadykov, I.A.; Silantiev, A.S.; Shamshin, I.O.; Aksenov, V.S.; Avdeev, K.A.; Frolov, F.S. Natural gas conversion and liquid/solid organic waste gasification by ultra-superheated steam. *Energies* **2022**, *15*, 3616. [[CrossRef](#)]
31. Frolov, S.M.; Smetanyuk, V.A.; Sadykov, I.A.; Silantiev, A.S.; Shamshin, I.O.; Aksenov, V.S.; Avdeev, K.A.; Frolov, F.S. Natural gas conversion and organic waste gasification by detonation-born ultra-superheated steam: Effect of reactor volume. *Fuels* **2022**, *3*, 375–391. [[CrossRef](#)]
32. Shindo, D.; Oikawa, T. *Analytical Electron Microscopy for Materials Science*; Springer: Tokyo, Japan, 2002. [[CrossRef](#)]
33. Fomenko, E.V.; Yumashev, V.V.; Kukhtetskiy, S.V.; Zhizhaev, A.M.; Anshits, A.G. Scanning electron microscopy—Energy-dispersive X-ray spectrometry (SEM–EDS) analysis of PM1–2 microspheres located in coal char particles with different morphologies. *Energy Fuels* **2020**, *34*, 8848–8856. [[CrossRef](#)]
34. Holder, C.F.; Schaak, R.E. Tutorial on powder X-ray diffraction for characterizing nanoscale materials. *ACS Nano* **2019**, *13*, 7359–7365. [[CrossRef](#)] [[PubMed](#)]
35. Lyu, F.; Thomas, M.; Hendriks, W.H.; van der Poel, A.F.B. Size reduction in feed technology and methods for determining, expressing and predicting particle size: A review. *Anim. Feed Sci. Technol.* **2020**, *261*, 114347. [[CrossRef](#)]
36. Sing, K. The use of nitrogen adsorption for the characterization of porous materials. *Colloids Surf. A Physicochem. Eng. Asp.* **2001**, *187–188*, 3–9. [[CrossRef](#)]
37. Rodríguez-Galván, A.; Contreras-Torres, F.F. Scanning scanning probe microscopy of biological structures: An elusive goal for many years. *Nanomaterials* **2022**, *12*, 3013. [[CrossRef](#)]
38. Demirbaş, A. Fuel characteristics of olive husk and walnut, hazelnut, sunflower, and almond shells. *Energy Sources* **2002**, *24*, 215–221. [[CrossRef](#)]
39. Binnig, G.; Rohrer, H. Scanning tunneling microscopy. *Helv. Phys. Acta* **1982**, *55*, 726–735.
40. Binnig, G.; Rohrer, H.; Gerber, C.; Weibel, E. Tunneling through a controllable vacuum gap. *Appl. Phys. Lett.* **1982**, *40*, 178–180. [[CrossRef](#)]
41. Binnig, G.; Quate, C.F.; Gerber, C. Atomic force microscope. *Phys. Rev. Lett.* **1986**, *56*, 930–933. [[CrossRef](#)]
42. Nyffenegger, R.M.; Penner, R.M.; Schierle, R. Electrostatic force microscopy of silver nanocrystals with nanometer-scale resolution. *Appl. Phys. Lett.* **1997**, *71*, 1878–1880. [[CrossRef](#)]
43. Hartmann, U. Magnetic force microscopy. *Annu. Rev. Mater. Sci.* **1999**, *29*, 53–87. [[CrossRef](#)]
44. Kalinin, A.S.; Atepalikhin, V.V.; Pakhomov, O.; Kholkin, A.L.; Tselev, A. An atomic force microscopy mode for nondestructive electromechanical studies and its application to diphenylalanine peptide nanotubes. *Ultramicroscopy* **2017**, *185*, 49–54. [[CrossRef](#)]
45. Maghsoudy-Louyeh, S.; Kropf, M.; Tittmann, B.R. Review of progress in atomic force microscopy. *Open Neuroimaging J.* **2018**, *12*, 86. [[CrossRef](#)]
46. Gregg, S.J.; Sing, K.S.W. *Adsorption, Surface Area and Porosity*; Academic Press: London, UK, 1982.
47. International Union of Pure and Applied Chemistry. Reporting physisorption data for gas/solid systems. *Pure Appl. Chem.* **1985**, *57*, 603. [[CrossRef](#)]
48. Brunauer, S.; Deming, L.S.; Deming, W.S.; Teller, E. On a theory of the van der Waals adsorption of gases. *J. Am. Chem. Soc.* **1940**, *62*, 1723. [[CrossRef](#)]

- 
49. Brunauer, S.; Emmett, P.H.; Teller, E. Adsorption of gases in multimolecular layers. *J. Am. Chem. Soc.* **1938**, *60*, 309–319. [[CrossRef](#)]
  50. Sharma, R.K.; Wooten, J.B.; Baliga, V.L.; Lin, X.; Chan, W.G.; Hajaligol, M.R. Characterization of chars from pyrolysis of lignin. *Fuel* **2004**, *83*, 1469–1482. [[CrossRef](#)]

**Disclaimer/Publisher’s Note:** The statements, opinions and data contained in all publications are solely those of the individual author(s) and contributor(s) and not of MDPI and/or the editor(s). MDPI and/or the editor(s) disclaim responsibility for any injury to people or property resulting from any ideas, methods, instructions or products referred to in the content.